

Characterization of Silicone Elastomer Seal Materials

A Major Qualifying Project
submitted to the faculty of Worcester Polytechnic Institute
in partial fulfillment of the requirements for the
Degree of Bachelor of Science in
Mechanical Engineering by

Leigh C. Duren
December 15, 2005

Advisors:

Prof. David Olinger
Worcester Polytechnic Institute

Patrick H. Dunlap, Jr.
National Aeronautics and Space Administration

Prof. Satya Shivkumar
Worcester Polytechnic Institute

Christopher C. Daniels, PhD
University of Akron



This document represents the work of the WPI student. The opinions expressed in this report are not necessarily those of the National Aeronautics and Space Administration or Worcester Polytechnic Institute

Abstract

The Advanced Docking Berthing System (ADBS) is being developed by NASA as part of new Exploration Initiative to develop an advanced mating system for future orbiting vehicles. Among other design challenges, the ADBS incorporates a seal-on-seal configuration rather than sealing conventionally against a flat surface. This project focused on three candidate seal materials of silicone elastomers. The silicone elastomers were mainly tested in the as-received condition to provide a means of comparison for tests performed after exposure to a simulated space environment. Of the many tests that will be performed before selection of a final seal material, the results presented here are for three main preliminary tests: compression set test, adhesion test between like elastomer materials, and Durometer measurements.

Compression set is a measurement expressed as a percentage of the amount of permanent deformation caused to the elastomer by compression. Based on compression set test in the as-received condition only, Silicone B exhibited the best resistance to permanent compression set while Silicone C experienced the most permanent compression set.

The adhesion test measures the amount of adhesion between two like elastomers, a concern for the seal-on-seal configuration of the ADBS. The adhesion test results revealed that, under the test conditions specified in Section 5.3.2, all three elastomers follow an increasing 3-Parameter Exponential Curve for adhesion stress with increased contact period.

The Durometer test measures the hardness of the elastomers using a comparison scale. The Durometer measurements show that the hardness of the elastomers increase with exposure to atomic oxygen as was predicted based on research. Although only two of the three candidate materials were tested, it is expected that the hardness of the third elastomer will increase with atomic oxygen exposure as well.

These results are essential preliminary results to the development of the sealing system for the ADBS. The final seal material will be chosen after many tests done at GRC and will be one that meets the seal and material requirements of the ADBS and does not lose its desired material properties with exposure to the space environment.

Acknowledgements

Professor Olinger- Professor Olinger is the director of the NASA Glenn MQP project center.

Professor Shivkumar- Professor Shivkumar was my elastomer specialist advisor and provided excellent feedback throughout the development of my project.

P.H. Dunlap, B.M. Steinetz, and C.C. Daniels- all served as mentors in one capacity or another making my experience at NASA a truly great one.

Table of Contents

1	Introduction.....	1
2	Background.....	3
2.1	National Aeronautics and Space Administration.....	3
2.1.1	Glenn Research Center	4
2.1.2	High Temperature Structural Seals and Thermal Barriers Research Team.....	6
2.2	Overview of NASA Glenn High Temperature Seal Development.....	7
2.3	Seal Development at NASA GRC for Advanced Docking Berthing Systems	11
2.3.1	Background on Docking Berthing Systems.....	11
2.3.2	Existing Systems.....	12
2.3.3	Seal and Material Requirements	14
2.4	Components of the Low Earth Orbital Environment.....	16
2.4.1	Atomic Oxygen.....	16
2.4.2	Ultraviolet Radiation and Vacuum Ultraviolet Radiation	16
2.4.3	Thermal Considerations	17
2.4.4	Simulated Space Environment.....	17
2.5	Low Earth Orbital Environment Interactions with Silicone Elastomers	18
2.6	Summary	20
3	Project Objective.....	21
4	Methodology for Elastomeric Material Evaluation	23
4.1	Phase I ADBS Seal Development.....	23
4.2	Elastomeric Material Evaluation.....	24
4.3	Compression Set Test	24
4.4	Small-Scale Flow Test	26
4.5	Adhesion Test	27
5	Results and Discussion	31
5.1	Elastomeric Material Evaluation.....	31
5.1.1	Silicone Elastomer A	31
5.1.2	Silicone Elastomer B.....	32
5.1.3	Silicone Elastomer C.....	33
5.1.4	Silicone Elastomer Summary.....	33
5.2	Compression Set Test	34
5.2.1	Compression Set of As-Received Elastomeric Seals.....	34
5.3	Adhesion Test	35
5.3.1	Adhesion Test Sample Attachment Method	36
5.3.2	Effects of Hold Time	38
5.3.3	Summary of Effect of Contact Period on Adhesion Stress.....	43
5.3.4	Optical Profilometry	45
5.4	Durometer Results	49
6	Conclusion	52
7	References.....	54
8	Appendix A.....	56

List of Figures

Figure 1: Locations of NASA Research Centers around the United States. (From: newemployee.nasa.gov/mycenter/default.htm)	4
Figure 2: Ceramic Wafer Seal.....	8
Figure 3: Braided Rope Seal.....	8
Figure 4: Unique Seal Test Apparatus at NASA GRC	10
Figure 5: Androgynous Peripheral Docking System (APAS) (Dunlap, 2005).....	12
Figure 6: Russian Probe (Dunlap, 2005).....	13
Figure 7: Passive Common Berthing Mechanism (PCBM) (Dunlap, 2005)	13
Figure 8: The Advanced Docking/Berthing System (ADBS) currently in progress	14
Figure 9: Earth's magnetic field with near earth orbits (NASA image).....	15
Figure 10: Compression Set Test Fixture	25
Figure 11: Compression Set Test Fixture Photograph.....	26
Figure 12: Small-Scale Flow Test Fixture.....	27
Figure 13: Blocking/Adhesion Test Fixture	29
Figure 14: Siloxane; the backbone of silicone elastomers.....	31
Figure 15: Micrograph (color enhanced) of Silicone A at 11.5X	32
Figure 16: Micrograph (color enhanced) Silicone B at 11.5X.....	33
Figure 17: Micrograph of Silicone C at 11.5X	33
Figure 18: Compression Set test results of o-ring specimens tested per ASTM Standard D395 (Test Method B).....	35
Figure 19: Chemical composition of common cyanoacrylates.....	36
Figure 20: Photograph of 0.375in. cylindrical adhesion sample attached with cyanoacrylate....	37
Figure 21: Effect of contact period on adhesion stress for Silicone A	40
Figure 22: Effect of contact period on adhesion stress for Silicone B.....	41
Figure 23: Effect of contact period on adhesion stress for Silicone C.....	42
Figure 24: Comparison of effect of contact period on adhesion stress between silicone elastomers	44
Figure 25: Silicone B sample representative of the surface contour of the adhesion samples.	46
Figure 26: Silicone A optical profile at 5X magnification	46
Figure 27: Silicone B optical profile at 5X magnification.....	47
Figure 28: Silicone C optical profile at 5X magnification.....	48
Figure 29: Durometer results for silicone elastomer compounds before and after AO exposure	50

List of Tables

Table 1: Physical properties of candidate seal materials	34
Table 2: Experimental fit curve constants for Silicone A.....	40
Table 3: Experimental fit curve constants for Silicone B.....	41
Table 4: Experimental fit curve constants for Silicone C.....	42

1 Introduction

This chapter begins by introducing the concept of the Advanced Docking Berthing System (ADBS) to be implemented by the National Aeronautics and Space Administration (NASA). An overview of the role of NASA Glenn Research Center (GRC) in the development of the ADBS is also given. Finally, the specific role of this Worcester Polytechnic Institute Project in the overall development of the ADBS is explained.

NASA is seeking to develop the ADBS to simplify and standardize the process of docking and berthing in space. This system will be androgynous to allow any two vehicles to dock together rather than having two complementary halves. In order to be androgynous the ADBS will incorporate a seal on seal interface which has not been incorporated into past docking berthing systems.

NASA GRC is in charge of the seal development while the main ADBS development is at the NASA Johnson Space Center (JSC). GRC is exploring possible elastomers to use in the seal application. Polymers are widely used in space vehicles including, but not limited to, structural materials, as in the case of the ADBS seal, thermal blankets, thermal control coatings, conformal coatings, adhesives and lubricants¹. The challenges that NASA GRC faces are developing a material that can meet the structural demand as well as stand up to the exposures of the space environment which can have detrimental effects on polymer chemical, electrical, thermal, optical, and mechanical properties.

This NASA sponsored, Worcester Polytechnic Institute project will assist NASA GRC in the development of sealing technology for the ADBS by testing candidate seal materials for their integrity in the ADBS seal application. The project includes the coordination of simulated space environment exposures to the candidate materials and tests on the candidate materials before and after exposure to the simulated space environment. Ultimately, the candidate materials will be evaluated on their performance and degradation due to exposure of the space environment.

2 Background

This chapter provides history on the mission and development of NASA and GRC. Within GRC, the team responsible for the seals of the ADBS is the Seals Team within the Mechanical Components Branch. Some of the past seal development projects are highlighted as well as current progress on the ADBS. The ADBS is also compared to older docking/berthing systems. The chapter ends with an explanation of some of the challenges for materials exposed to low earth orbit environment (LEO).

2.1 National Aeronautics and Space Administration

NASA was created on October 1, 1958 as “*an Act to provide for research into the problems of flight within and outside the Earth’s atmosphere, and for other purposes*”². Although the inception of NASA was directly related to the demands of national defense, the technology that NASA has developed has proved useful for many other functions. For example NASA’s Landsat program has been used for crop management, fault line detection, and weather tracking. The current mission statements of NASA are:

- To advance and communicate scientific knowledge and understanding of Earth, the solar system, and the universe;
- To advance human exploration, use, and development of space;
- To research, develop, verify, and transfer advanced aeronautics, space, and related technologies³.

NASA was formed from the National Advisory Committee for Aeronautics (NACA), the Langley Aeronautical Laboratory, Ames Aeronautical Laboratory, and the Lewis Flight Propulsion Laboratory. Shortly after its inception, NASA incorporated the Naval Research Laboratory in Maryland, the Jet Propulsion Laboratory at the California Institute of Technology for the Army, and the Army Ballistic Missile Agency in Alabama. From here NASA grew and now includes ten major centers around the United States shown in Figure 1 below.

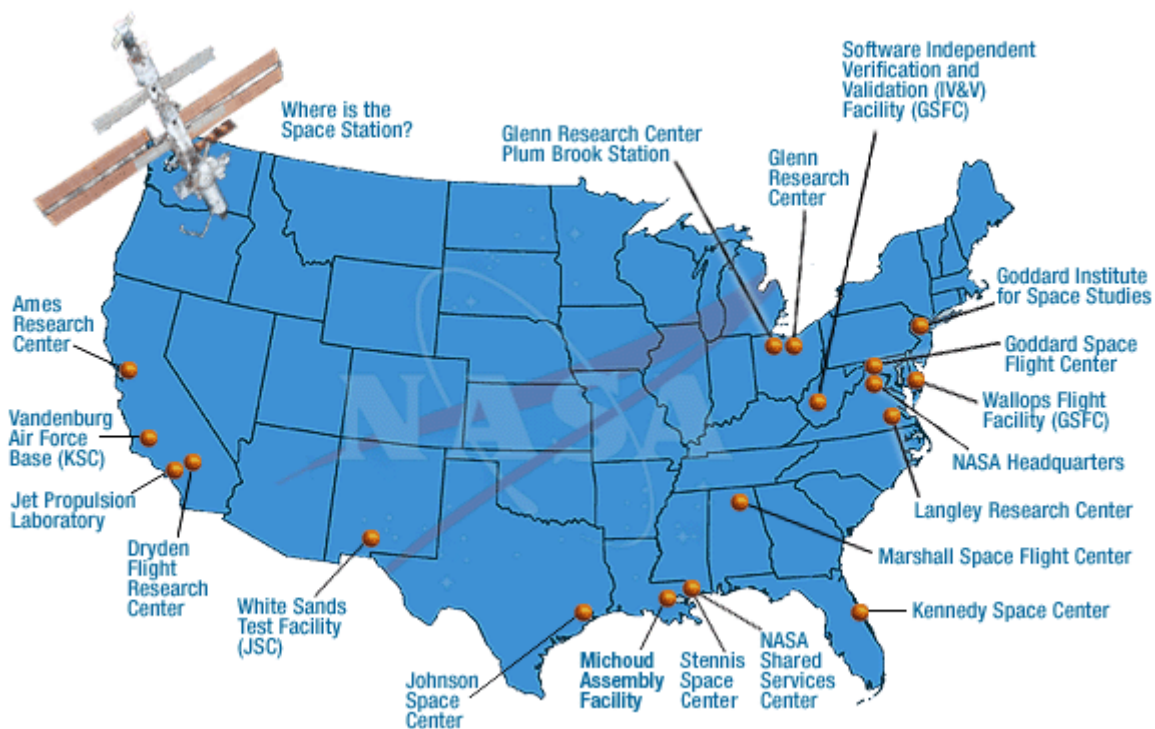


Figure 1: Locations of NASA Research Centers around the United States. (From: newemployee.nasa.gov/mycenter/default.htm)

2.1.1 Glenn Research Center

What is now known as Glenn Research Center (GRC) was once the Lewis Flight Propulsion Laboratory. The Lewis Flight Propulsion Laboratory was established in Cleveland, Ohio, on January 23, 1941 by the National Advisory Committee for Aeronautics (NACA). When NASA

was born in 1958, and NACA dissolved, Lewis Flight Propulsion Laboratory was renamed the NASA Lewis Research Center. In 1999 the Lewis Research Center was officially renamed the NASA John H. Glenn Research Center at Lewis Field to recognize the contributions to space exploration and technology of both John H. Glenn, and George W. Lewis. Among their many other accomplishments, Glenn was the first American to orbit the earth and Lewis was the Director of Aeronautical Research from 1924-1947 for NACA⁴.

Today, GRC focuses mainly on technological developments in the areas of power, propulsion, communications, and microgravity science. GRC is a 350-acre campus with over 150 buildings containing world class research facilities. These include five wind tunnels, the Aero-Acoustic Propulsion Laboratory, the Engine Components Research Laboratory, the Propulsion Systems Laboratory, and the Engine Research Building. Also a part of GRC is Plum Brook Station in Sandusky, Ohio 50 miles away from Cleveland. Plum Brook Station is a 6400-acre facility that houses a Hypersonic Tunnel Facility, Space Power Facility, Spacecraft Propulsion Research Facility, and the Cryogenic Propellant Tank Facility.

One sector of GRC is the Structures Division which includes the Mechanical Components Branch. The mission of the Mechanical Components Branch is to “perform research and development in mechanical components and system technologies to improve the performance, reliability, and integrity of aerospace drive systems, high temperature seals, and space mechanisms⁵.” Within the Mechanical Components Branch of GRC is the Structural Seals and Thermal Barriers Research Team which works in collaboration with all NASA sites in the development of high temperature seals for aerospace applications.

2.1.2 High Temperature Structural Seals and Thermal Barriers Research Team

The mission of the structural seals team at NASA GRC is to “develop unique seals for extreme temperature engine, hypersonic vehicle, and rocket applications⁶”. More specifically the seals team seeks to:

- Develop advanced structural seals capable of extreme (1500–3500°F/815-1927°C) temperatures;
- Exploit novel design techniques to meet leakage, durability, and resiliency (spring-back) goals across operating temperature range;
- Evaluate seal performance through compression, flow and extreme thermal tests;
- Develop/validate analytical models to predict leakage and resiliency performance;
- Demonstrate seal performance through prototype engine tests.

The Seals Team at NASA GRC has made many advances in high temperature seal technology, even winning NASA’s 1996 Government Invention of the Year for their high temperature, flexible, fiber performance seal created by Dr. Bruce Steinetz, Mechanical Components Branch NASA GRC, and Paul Sirocky (retired). High temperature seal development is crucial to the development of future space vehicles not only in the area of berthing docking, but also to reduce aircraft emission and improve fuel consumption efficiency. The lessons learned from past seal developments will aid in the development of the seals for the ADBS.

2.2 Overview of NASA Glenn High Temperature Seal Development

At the 2003 NASA Seal/Secondary Air System Workshop a presentation on the overview of NASA Glenn seal developments was presented. This section summarizes the developments of only structural seals although the workshop reviewed development in turbine seals and clearance management as well.

At the time of the workshop the NASA GRC Structural Seals team was working on the Next Generation Launch Technology (NGLT) Program. The goals of the NGLT program were to develop hot (2000-2500+°F/1093-1371°C), flexible, dynamic structural seals for ram and scramjet propulsion systems as well as to develop reusable re-entry vehicle control surface seals to prevent ingestion of hot (6000°F/3316°C) boundary layer flow. The seals were determined to be critical to meeting the NGLT program life, safety and cost goals⁷.

High temperature structural seal development began in the late 1980s where GRC was the prime sector of NASA for high temperature structural seal development. Two of the major developments earlier in the seals discipline were the ceramic wafer seal and the braided rope seal⁸.

The ceramic wafer seal, Figure 2, boasts a high operation temperature of 2500°F (1371°C), low leakage and sufficient flexibility derived from the sliding of adjacent wafers to conform to wall distortions. It was also beneficial to high temperature seal development because the ceramic material had a lighter weight than the metal predecessors.

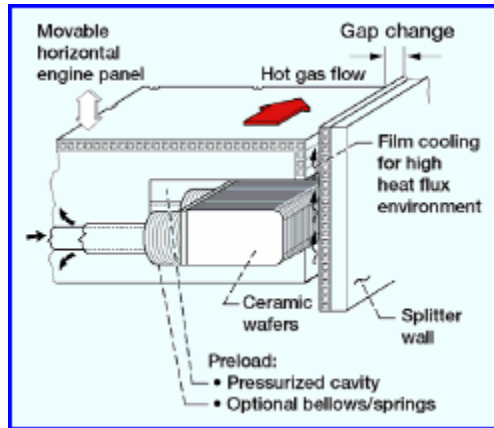


Figure 2: Ceramic Wafer Seal

The braided rope seal, Figure 3, has been developed for high temperature operations where the seal is needed and designed to serve both as a seal and to accommodate mounts to allow for relative thermal growth between high temperature, brittle primary structures as well as the surrounding support structures. These braided rope seals incorporate a ceramic core with a superalloy wire sheath or are made of completely ceramic fibers.

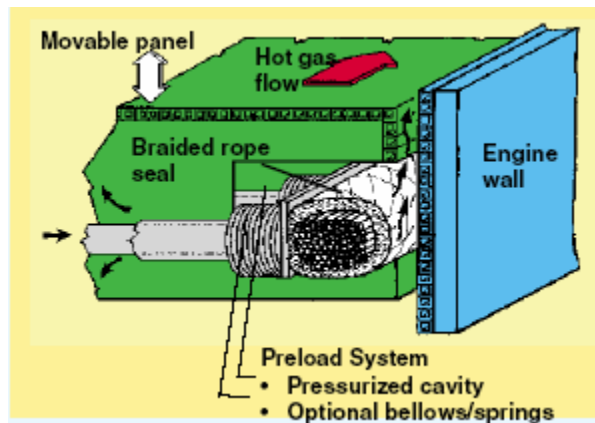


Figure 3: Braided Rope Seal

These two seals, the ceramic wafer seal and braided rope seal, were the starting point for the seal concept development and testing planned for NASA's 3rd Generation high temperature seal development tasks.

NASA GRC has also developed a unique testing apparatus, Figure 4, to evaluate seal performance. The equipment can simulate the temperatures experienced during space missions (notice the 3000°F (1649°C) furnace), loads, and scrubbing conditions that the seals will endure. The compression test fixture (upper left photo Figure 4) is used to assess seal load versus linear compression, preload, and stiffness at temperature. The scrub test fixture (middle photo Figure 4) is used to assess seal wear rates and frictional loads. The seal testing apparatus is unique to NASA GRC and includes multiple load cells with multi-ranging capabilities for accurate load measurements, dual servo-valves to allow for precise testing at various stroke rates, and a non-contact laser extensometer system to measure displacement.

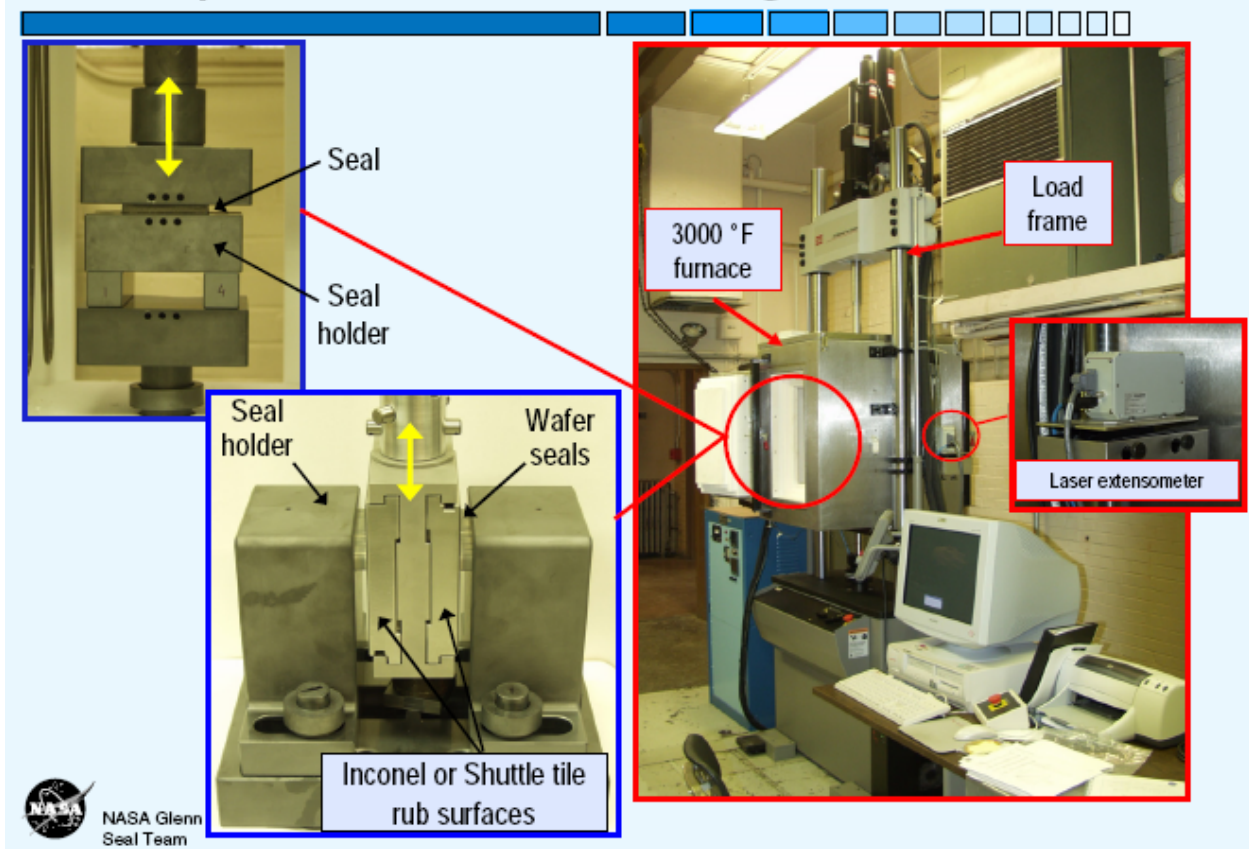


Figure 4: Unique Seal Test Apparatus at NASA GRC

The ADBS project has taken the structural seals team in a new direction. Instead of developing ceramic and superalloy seals, the current focus of the seals team is developing an elastomeric or metallic seal that will incorporate a seal on seal interface. The metallic seal option is only mentioned here as a possible solution for the ADBS seal since this project focused only on elastomeric seal development.

2.3 Seal Development at NASA GRC for Advanced Docking Berthing Systems

With the lessons learned in past seal developments, NASA GRC is working to develop seals for the ADBS in conjunction with NASA JSC. The mechanism by which docking and berthing occurs, along with the three docking systems that are currently in use, are explained in this chapter. In order to make the ADBS a success, a structural seal material must be identified to meet the needs of the ADBS.

2.3.1 Background on Docking Berthing Systems

The ADBS is part of a new Exploration Initiative to develop an advanced mating system for future orbiting vehicles. Berthing refers to mating operations where an inactive module or vehicle is placed into the mating interface using a Remote Manipulator System (RMS), while docking refers to mating operations where an active vehicle flies into the mating interface under its own power⁹. JSC is designing the ADBS to allow vehicles to dock at lower velocities as well as be androgynous so that any two vehicles can attach to each other.

GRC is addressing several challenges of the system from the sealing standpoint. In order for the new system to be androgynous, there must be a seal-on-seal configuration. Generally, O-ring type seals are used against flat surfaces to provide successful sealing, but the ADBS will require seals to seal against each other. While the seal-on-seal configuration is one challenge, the seals will also experience exposure to the space environment while in transit to and from earth and in orbit. The seals must withstand this exposure with minimal degradation in performance.

2.3.2 Existing Systems

There are three existing docking berthing systems. The existing systems have unique active and passive halves which do not allow for vehicle-to-vehicle mating if two of the same halves are present. Current elastomeric seals typically seal against metal surfaces and are not exposed to space environments for long periods of time. Each system is shown below: the Androgynous Peripheral Docking System (APAS) (Figure 5), Russian Probe (Figure 6), and the Passive Common Berthing Mechanism (PCBM). The APAS is used in the International Space Station (ISS) missions. The Russian Probe was developed by the Russian Space Corporation Energia and the PCBM is a generic device which has been used to join segments of the ISS. The passive half is shown in Figure 7; the active and passive halves together can maintain a pressurized atmosphere to allow astronaut passage as well as providing a structural linkage between elements¹⁰.

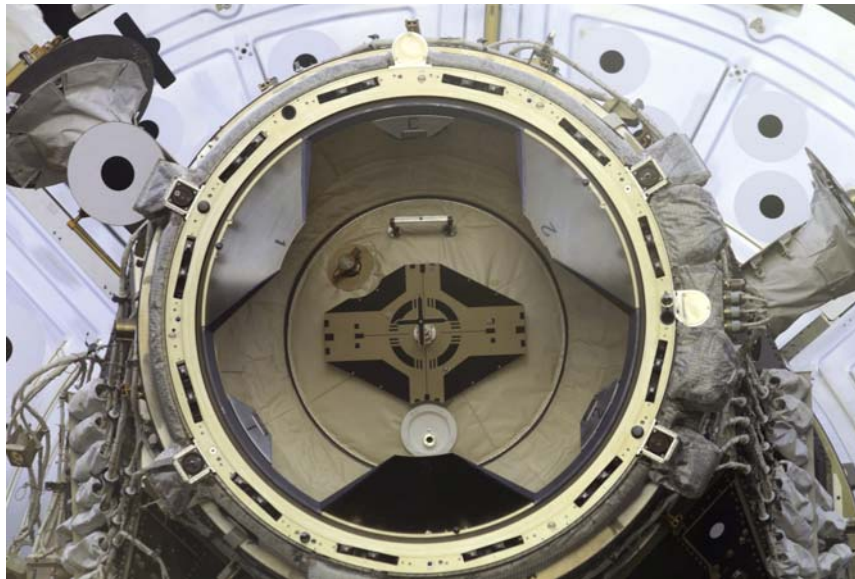


Figure 5: Androgynous Peripheral Docking System (APAS) (Dunlap, 2005)

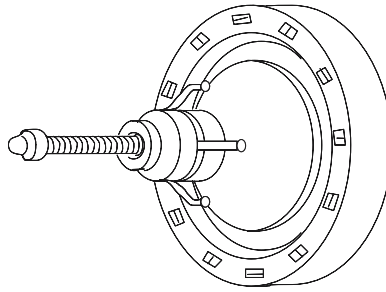


Figure 6: Russian Probe (Dunlap, 2005)

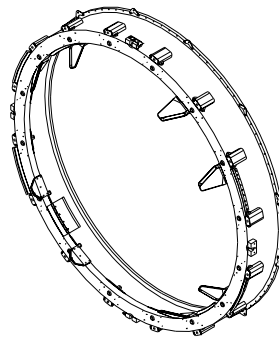


Figure 7: Passive Common Berthing Mechanism (PCBM) (Dunlap, 2005)

The ADBS, shown in Figure 8, is the docking system under design. Presently at GRC, the Seal Team is testing candidate elastomers that can withstand seal-on-seal interfaces and the space environment.

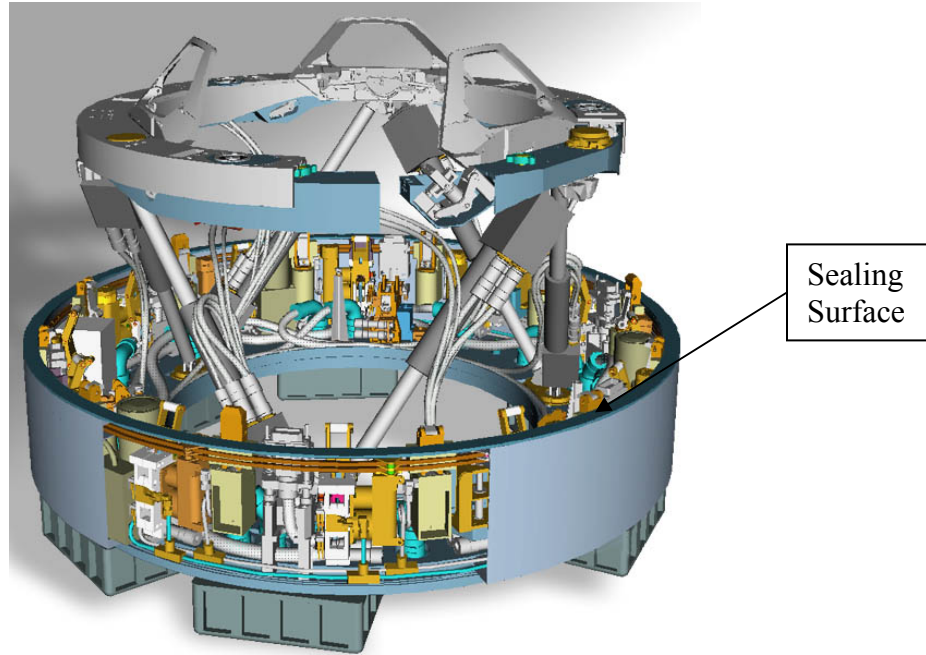


Figure 8: The Advanced Docking/Berthing System (ADBS) currently in progress

2.3.3 Seal and Material Requirements

There are four key requirements for ADBS seals:

- Integrate a seal-on-seal configuration.
- Allow no more than (0.044lbm per day) of air leakage.
- Endure exposures to the LEO environment, as well as the environment experienced during transit to and from the Moon and Mars, without compromising the integrity of the seal.
- Withstand a wide range of temperatures (-50 to 50°C / -58 to 122°F) and retain its desired materials properties.

The mechanical design of the ADBS will determine its structural requirements, but the environment it is exposed to will play a large role in the elastomer selection. The near earth

environment is separated into three general parts known as the LEO, mid-earth orbit (MEO), and geosynchronous earth orbit (GEO) shown in Figure 9.

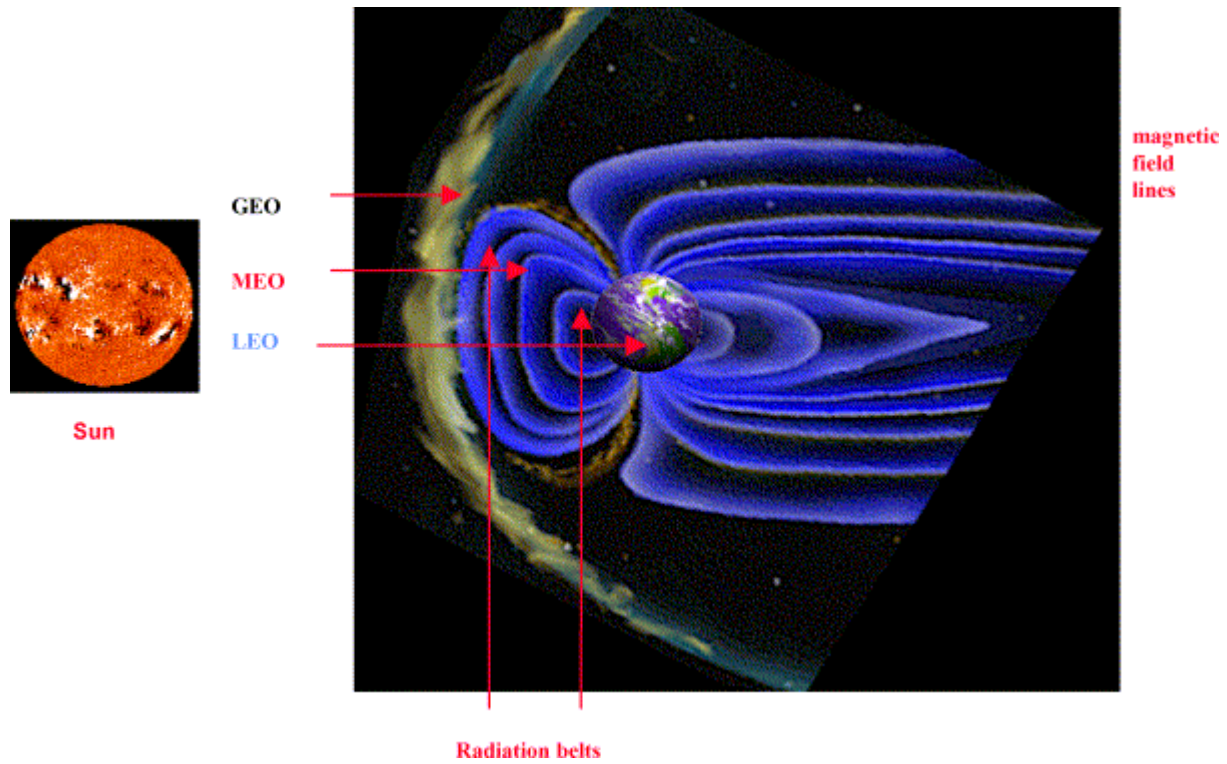


Figure 9: Earth's magnetic field with near earth orbits (NASA image)¹¹

The MEO environment, with altitudes ranging from 1200-35700km (746-22183miles) includes the inner trapped radiation belt and the outer belt consisting primarily of high-energy protons to low to moderate energy electrons. The GEO environment, at an altitude of about 36,000km (22369miles), has a radiation environment primarily of electrons. However, the LEO, with altitudes ranging from approximately 200-1200km (124-746miles), is of main concern for orbiting vehicles.

2.4 Components of the Low Earth Orbital Environment

The LEO is considered to be the atmosphere around the earth below about 1000km (621miles)¹².

The LEO is like no atmosphere on earth which creates challenges in the development of spacecraft materials. The following section explains the major components of the LEO and their individual threats specific to polymers. It is important to note, however, that the combined effects of the LEO constituents can have even harsher effects on polymers.

2.4.1 Atomic Oxygen

Atomic oxygen (AO) is the predominant species of LEO, especially between the altitudes of 180 to 640km (112 to 398miles)¹³. Atomic oxygen is formed when short wavelength ultraviolet radiation ($>5.12\text{eV}$, $<243\text{nm}$) from the sun dissociates molecular oxygen in the upper atmosphere. The neutral oxygen atoms that are formed have very large mean free paths (10^4m at 400km/6.2miles at 250miles); large mean free paths mean a very low probability of re-association. When atomic oxygen atoms collide with space vehicles the following reactions can occur: chemical reactions with surface atoms, elastic scattering, scattering with partial or full thermal accommodation, or recombination can occur. Typically, LEO orbiting vehicles move with a velocity of about 7.7km/sec (4.8miles/s) and “ram” into atomic oxygen with enough energy (on average 4.5eV) to break the chemical bonds of polymers¹⁴. The term ram atomic oxygen is used to refer to the atomic oxygen hitting the ram surfaces of space vehicles¹⁵.

2.4.2 Ultraviolet Radiation and Vacuum Ultraviolet Radiation

Ultraviolet radiation (UV) and vacuum ultraviolet radiation (VUV) are energetic enough to break the bonds of polymers such as the C-C and C-O groups. The total energy that the sun provides to

the atmosphere is 1366W/m^2 (127W/ft^2), known as the solar constant, while the UV radiation is only about 8% of this energy or 110W/m^2 (10.2W/ft^2). At the near ultraviolet (NUV) range, or 200-400nm, the photons' energy is $E_{\text{ph}} > 3\text{eV}$, while for VUV, or below 200nm, the photons' energy increases to $E_{\text{ph}} > 5\text{eV}$. UV radiation can cause degradation of thermo-optical properties while VUV effects are characterized by energy loss processes of bond breaking and excitations by no direct atomic displacements. The synergistic effect of UV and AO is more detrimental to degradation of polymers than either constituent alone.

2.4.3 Thermal Considerations

Spacecraft are coated with materials in order to regulate the temperature and protect the craft while maintaining a reasonable weight. The seals for the ADBS system will be exposed to the space environment and the thermal gradients associated with space travel. The heat load on spacecraft is primarily due to direct solar illumination, and also includes heat radiated from the earth. JSC has calculated that the ADBS seals will only be exposed to operating temperatures ranging from -50°C to 50°C (-58°F to 122°C), while other parts of the space vehicle may be exposed to a much wider range of temperatures. The temperature range for the seals is quite limiting for elastomeric seal selection as will be discussed in Section 5.1. The seal material for the ADBS must be able to maintain its structural integrity and resiliency throughout its lifetime.

2.4.4 Simulated Space Environment

In order to simulate the space environment, NASA GRC has an AO Beam Facility in the Electro-Physics Branch. The AO beam apparatus can simulate AO, VUV, and thermal fluxes all

together, or any combination of the three space environment constituents. The AO beam apparatus can accommodate samples up to 30cm² (12in²). The AO exposure flux is accelerated and ranges from 10¹⁵ to 10¹⁷atoms/cm²s (6548 to 6561atoms/in²s). The VUV source is a deuterium lamp which provides wavelengths from 115 to 200nm with an intensity equivalent to 3 to 5 suns. Lastly, the AO beam apparatus is able to provide elevated thermal conditions. The AO Beam Facility at NASA GRC is very important to simulate the environment that the ADBS seals will be exposed to.

2.5 Low Earth Orbital Environment Interactions with Silicone Elastomers

Because atomic oxygen is a predominant species in the LEO, this section provides a more in depth examination of the interaction of AO with silicone elastomers. Silicone elastomers are the only class of polymers being considered for the ADBS seal, as is explained further in the Results and Discussion Chapter.

Silicone elastomers are quite unique in that they do not chemically erode with AO exposure like other organic materials. Instead, silicones react with AO and form an oxidized, hardened surface layer caused by the loss of methyl groups¹⁶. The reaction between AO and silicone produces SiO_x, where x is close to 2 and SiO₂ is silica.¹⁷. The oxidized layer increases in thickness and hardness with exposure to AO which has been measured using nanomechanical hardness testing, a depth-sensing indentation testing in the submicrometer range.

The near-silica layer that is formed is an atomic-oxygen resistant layer which protects the underlying material. Silicones have been used to protect polymers from AO erosion but the effectiveness depends on the depth of the surface cracks caused by tension and the depth of the

oxygen diffusion from the near silica surface to the silicone interior¹⁸. The near-silica layer is in tension due to the loss of methyl groups. The loss of the methyl groups also poses the potential for oxygen diffusion from the oxidized surface layer to the interior, be it another material or unexposed silicone. In order to fully utilize the benefits of the AO resistant silica surface, methods have been proposed to decrease or eliminate surface cracking.

It has been proposed that rougher silicone surfaces crack less than smooth surfaces when reacting with AO. The surface tension causing cracking can be a result of the shrinkage magnitude increasing, transition region thickness, and/or Durometer hardness. The transition region is defined as the depth where tension due to AO changes from the surface tension to that of unexposed silicone (i.e., zero). The Durometer hardness effects the cracking because a softer material can absorb more stress in the transition region. It is believed that while a flat, smooth surface can only relieve tension by pulling the surface apart, a rough surface is able to release tension by flattening of the rough surface. However, a surface that is too rough can also cause cracking. In order to define the correct surface roughness, a semi-quantitative analysis has been undertaken in more detail in Reference 18. A brief description of this method follows: The surface roughness can be considered as a number of near flat surfaces. If these near flat surfaces are too large, the near flat surfaces become large enough to be considered smooth surfaces and the tension will be large enough to cause cracking. The surface roughness must be greater than the oxygen penetration depth, otherwise the shrinkage and the stress would penetrate the region under the rough part of the surface and the rough surface would not be sufficient enough to absorb all the tension stresses.

Silicone has been widely used in space applications including use as potting compounds, adhesives, seals, gaskets, hydrophobic surfaces, and the afore mentioned atomic oxygen protective coatings. However, the use of moderate to high volatility silicones in the LEO has resulted in silicone contamination of silica deposits on other surfaces which are simultaneously being exposed to AO¹⁹. This becomes a significant problem because silica deposits become fixed to the surface and are unable to reevaporate. The elastic modulus of the silicone contaminants approaches that of fused silica with increasing atomic oxygen fluence^a. Most notably, silicone contamination was determined to be the problem of greatest widespread interest according to a survey response in the 8th International Symposium on “Materials in a Space Environment” held in Arcachon, France in June of 2000²⁰. This is a specific concern for the flexible metallic seals which are backed by a silicone elastomer. Silica deposits on the metallic sealing surface could potentially cause permanent deformation to the sealing surface during compression resulting in paths for leakage.

2.6 Summary

In order to develop an effective sealing material for the ADBS, the elastomer must be able to meet the requirements explained in this chapter as well as maintain the desired material properties after long exposures to the LEO and thermal gradients. These guidelines are used for a specific project statement that focuses solely on the material requirements for the ADBS.

^a It should be noted here that fluence is integrated flux expressed in units of particles or energy per unit area while flux is expressed as particles or energy per unit area time.

3 Project Objective

The Seal Team at GRC devised a project plan to evaluate candidate seal materials for the ADBS application. The plan included exposing candidate seal materials to simulated space environments and evaluating their performance before and after exposure. In order to assist in the development of the ADBS this Worcester Polytechnic Institute project sought generally to accomplish the following:

- Research on properties for candidate elastomeric seal materials;
- Perform tests on seals and materials before and after exposure to evaluate performance and degradation due to exposure^b

The research on material properties of candidate elastomeric seals was important because it enabled the research team to make accurate predictions on the behavior of the elastomeric seals.

This project focused on three main tests: compression set test, adhesion test, and Durometer tests. The majority of these tests were performed on the silicone elastomers in the as-received condition to provide NASA GRC with baseline data. The baseline data is important data that can be used to determine how test results change with exposure to the simulated space environment.

The compression set test, a measurement of permanent deformation due to compressive forces, was important so that the effects of the simulated space environment on compression could be compared quantitatively to compression set in the as received condition. The objective of the adhesion tests was to determine the amount of adhesion between like elastomers with a long term objective to determine if adhesion increases or decreases with exposure to the simulated space environment. Finally, the objective of the Durometer test, a measurement of hardness on a

^b From Research Position Summary provided by Patrick H. Dunlap, Jr. at NASA GRC

comparative scale, was to determine how hardness changed with exposure to the space environment.

4 Methodology for Elastomeric Material Evaluation

This ADBS project has been an ongoing project at NASA GRC. The following section explains the working plan that the seal team at GRC developed and methods of testing that will be used to select the seal material. It should be noted that this section explains all of the preliminary tests that the Seals Team will be performing on the candidate seal materials, while this project only focused on the compression set test, adhesion test, and Durometer test.

4.1 Phase I ADBS Seal Development

Before the start of this project, the Seals Team at GRC had already started on the development of ADBS seal and performed the following:

- Reviewed lessons learned from seals on existing docking/berthing systems (e.g., Shuttle, ISS) and identified issues to address for ADBS;
- Reviewed previous ADBS seal development;
- Defined seal design requirements;
- Selected seal materials and designs to evaluate both elastomeric and metallic seals
- Formulated test plan including simulated space environment exposures (i.e., atomic oxygen, UV radiation);
- Designed and fabricated test fixtures for seal evaluations before and after simulated space environment exposures:
 - Compression set test fixture;
 - Blocking/adhesion test fixture;
 - Small-scale flow fixture.

4.2 Elastomeric Material Evaluation

Material evaluation measured material properties including Durometer (a comparative hardness scale), operational temperature range, composition, and surface quality. A high Durometer, i.e., comparatively hard material, requires more clamping force from the ADBS. The operational temperature range narrowed down which elastomer compositions are suitable for the ADBS application, among other things such as resistance to AO. Surface quality and consistency is important to the overall sealing effectiveness of the material.

4.3 Compression Set Test

The compression set test, shown in Figure 10 and Figure 11, was used to measure the compression set of the elastomeric O-rings. Compression set is measured as the ratio of thickness after compression to initial thickness and is expressed as a percentage. Compression set measures the amount of permanent deformation caused by compressive forces. Deformation is caused by a combination of physical and chemical processes caused by the compression necessary for sealing. Of course the physical process is reversible and involves the motion of chains towards new equilibrium configurations in the strained state. The new equilibrium is obtained by the movement of entanglements and relaxation of dangling ends. The irreversible chemical process which causes permanent compression set involves scission and cross-linking from the breakage and formation of covalent bonds²¹. This test conforms to ASTM D 393-03 Test Method B (constant deflection in air) and can accommodate O-ring seals up to 12in (30cm) in diameter or multiple smaller diameter seals²². The compression set tests reported in this

research were done in the as-received condition, but will also be done before and after UV and AO exposure to indicate if there is any loss in sealing effectiveness due to compression set.

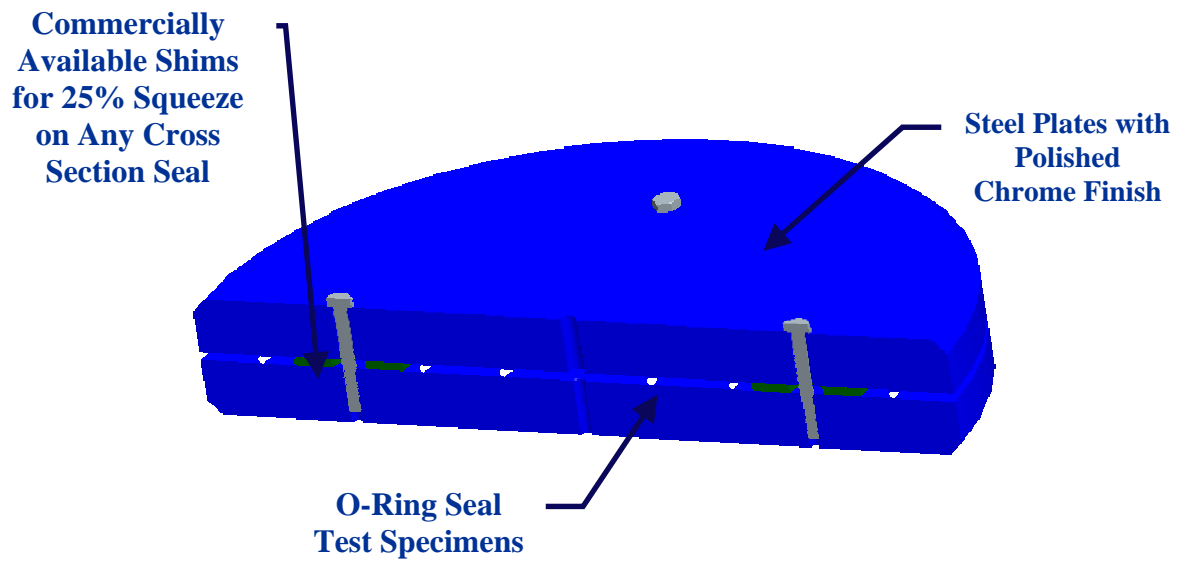


Figure 10: Compression Set Test Fixture



Figure 11: Compression Set Test Fixture Photograph

4.4 *Small-Scale Flow Test*

The small-scale flow test, see Figure 12, was not performed in this research, but will be used in determining the final seal material so it is important to mention. The small-scale flow test measures leak rates for the elastomeric seals, for the ADBS. The fixture produces an accurate representation of atmospheric-to-vacuum condition across the seals. Leakage can be determined accurately using the pressure decay method while the leakage past the vacuum side O-ring seals does not alter or interfere with the test measurements. The pressure decay method uses a pressure vessel with a known volume and pressure of gas and measures the leakage through the O-ring seal. This test gives a leakage rate of mass per unit time.

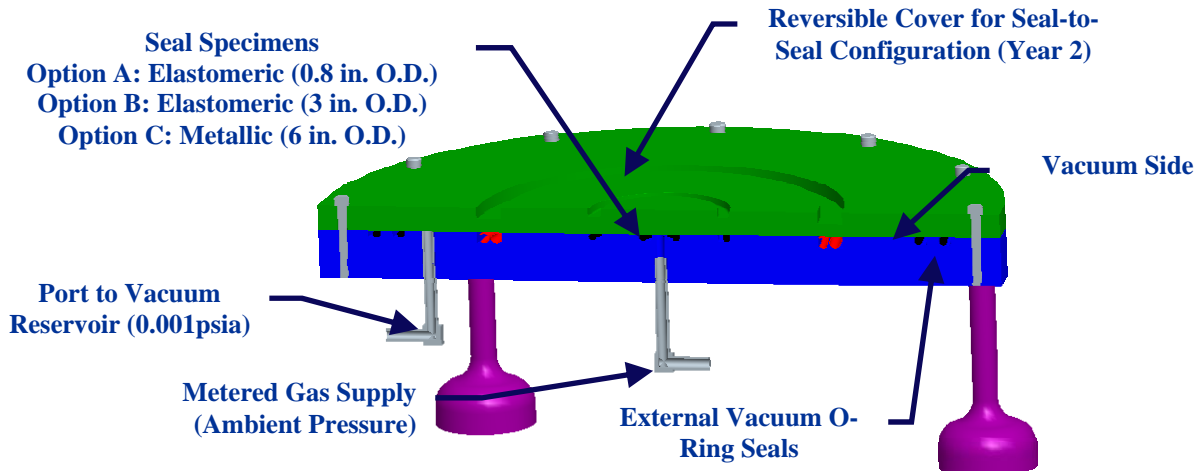


Figure 12: Small-Scale Flow Test Fixture

4.5 Adhesion Test

The adhesion test, Figure 13, evaluates the amount of adhesion between two elastomeric test samples. The test generates stress versus displacement data in both compression and tension. The test objective, equipment, and generic procedure are described in this section.

The adhesion test is necessary in designing the ADBS to detect the amount of adhesion between the two elastomer seal materials. From this adhesion test, the amount of adhesion force between the two halves of the ADBS can eventually be calculated. The seals on the ADBS will be rounded, so the conversion to full scale adhesion force is not exactly proportional. The adhesion between elastomer seals could potentially bond the spacecraft together under the compression forces imposed while the spacecrafts are mated. The system must be designed with mechanisms to overcome the adhesion force and separate the two vehicles and the seals must be manufactured to be held securely in place on their respective space vehicles during separation.

The test fixture was designed based on specifications from ASTM D3354-96 for Blocking Load of Plastic Film by the Parallel Plate Method which measures “the degree of blocking (unwanted adhesion) existing between layers of plastic film”²³. The Seals Team adhesion test measures the adhesion between two elastomers of approximately 0.5cm (0.20in.) in thickness. ASTM D-3354 expresses the blocking load in grams causing two layers of polyethylene film to separate with an area of contact of 100cm² (15.5in²), while the Seals Team adhesion is expressed in stress to account for any variability in sample size.

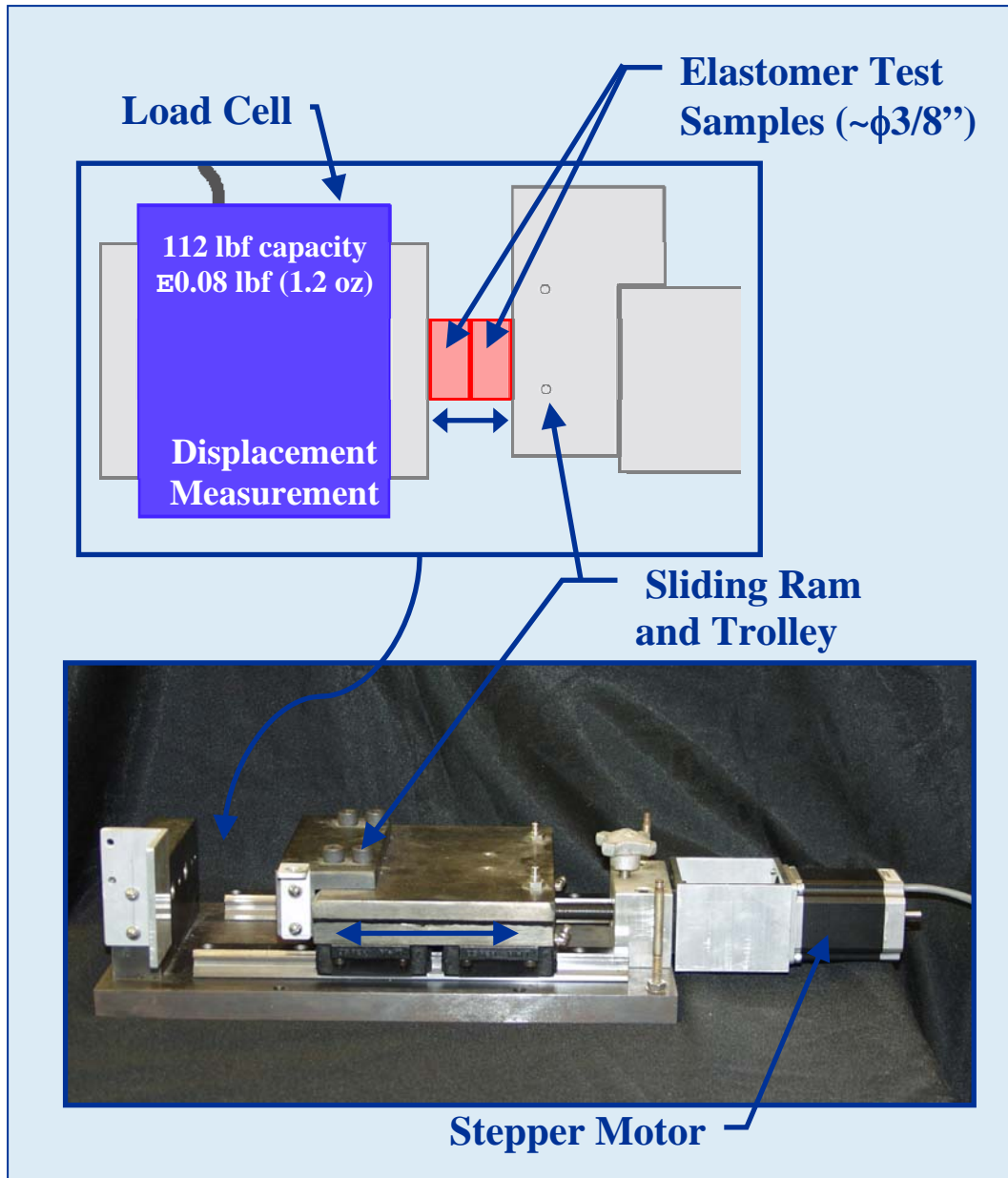


Figure 13: Blocking/Adhesion Test Fixture

The test fixture is powered by a Techtronix PS280 DC Power Supply to a stepper motor. The motor provides movement for the compression, hold time, and separation of the test samples. Displacement of the samples is measured by a linear variable differential transformer (LVDT) while compression and adhesion forces are measured by an Interface load cell with a 56lbf

(249N) capacity. A LabView program is coupled with the test fixture and serves as a control and data acquisition program.

To perform the adhesion test, one sample is fixed to the load cell and one to the trolley. The load cell is stationary while the stepper motor moves the trolley. Sample alignment was designed into the test fixture during the manufacturing of the test fixture by aligning the holes on the load cell and trolley for the mounting buttons. Using LabView7.1 the following parameters are entered into the adhesion test program: sample thicknesses, sample diameters, load speed, hold time, unload speed, and compression percentage. The program brings the elastomers samples together and begins recording data as soon as a load of 0.02lbf (.089N) is detected by the load cell. The force data is then collected in each of the three adhesion test stages: load, hold, and unload. Compression forces yield negative sign readings while tension forces yield positive values. The LVDT measurements ensure that the sample is being compressed to the specified percentage during the hold time. To ensure experiment repeatability an Adhesion Test Operator Check Sheet was created and is located in Appendix A.

5 Results and Discussion

5.1 Elastomeric Material Evaluation

Elastomers come in many different classes such as butyl—known for its extremely low permeability, ethylene polypropylene—known for its excellent resistivity to polar solvents, and fluorocarbons—one of the most widely used seal materials in the world, but silicone is the only elastomer class that offers resistance to AO as well as retains its material integrity in the operating temperature range of the ADBS (-50 to 100°C / -58 to 212°F) . The main backbone of the silicone elastomer is siloxane, shown in Figure 14, where pink, orange, red, and grey represent silicone, oxygen, carbon, and hydrogen respectively. In chemical terms, siloxane is R_2SiO where R_2 is an alkyl group.

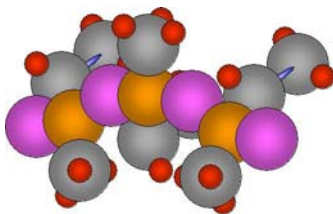


Figure 14: Siloxane; the backbone of silicone elastomers²⁴

Three different silicone elastomers were tested, all obtained from large commercial elastomer manufacturers. The manufacturer specified properties are presented below for each elastomer.

5.1.1 Silicone Elastomer A

Silicone Elastomer A, here after referred to as Silicone A, is a silicone elastomer of 70 ± 5 Durometer hardness on the Shore M Scale. The recommended operating temperature range is -175 to 400°F (-115 to 204°C). According to the manufacturer data sheet, it has a tensile strength of 1240psi (8.54MPa), percent elongation of 242% and a specific gravity of 1.27. It is

recommended by the manufacturer for use with ozone, weather resistance, and extreme low temperatures among other applications.

The material is homogenous in color to the naked eye. The surface of Silicone A was inspected using an optical microscope attached to a digital camera. Figure 15 is a photograph of a random area of Silicone A. The sample surface was cleaned before photographing with 99% Isopropyl Alcohol, the manufacturer recommended solvent for cleaning. This photograph shows there is variation in surface color indicating possible variation in surface composition. The darker string-like coloration is visible with the naked eye and is perhaps material contamination.

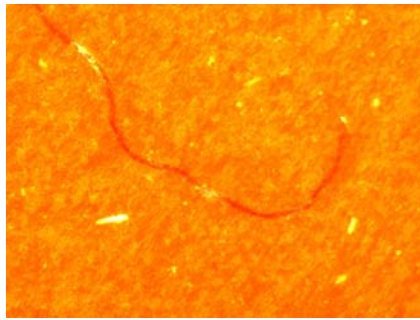


Figure 15: Micrograph (color enhanced) of Silicone A at 11.5X

5.1.2 Silicone Elastomer B

Silicone Elastomer B (Figure 16), here after referred to as Silicone B, is a silicone elastomer of 50 ± 5 Durometer hardness on the Shore M hardness scale with a manufacturer recommended operating temperature range of -103 to 400°F (-75 to 204°C). It has a tensile strength of 974psi (6.71MPa) and a percent elongation of 414% . It is recommended by the manufacturer for use with ozone, weather resistance, and low temperatures among other applications.

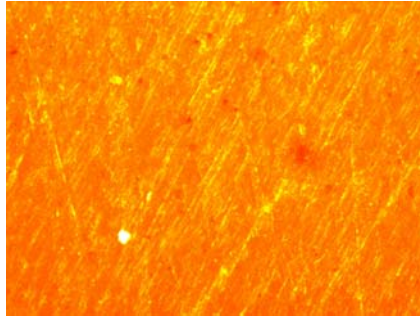


Figure 16: Micrograph (color enhanced) Silicone B at 11.5X

5.1.3 Silicone Elastomer C

Silicone Elastomer C (Figure 17), here after referred to as Silicone C, was provided by a different manufacturer than Silicone A and Silicone B. Silicone C has a hardness of 38 on the Shore M hardness scale. The brittle point, the point at which the elastomer will no longer perform in the current state, of Silicone C is -117°F (-83°C). The manufacturer specifies the tensile strength as 1050psi (7.23MPa), percent elongation as 625% and a specific gravity of 1.13.



Figure 17: Micrograph of Silicone C at 11.5X

5.1.4 Silicone Elastomer Summary

A summary of the manufacturer specified properties is provided in below for a total comparison of all three elastomers.

	Silicone A	Silicone B	Silicone C
Hardness (Shore M)	70±5	50±5	38
Recommended Operating Temperatures (°F)	-175 to 400	-103 to 400	-117 Brittle Point
Tensile Strength (psi)	1240	974	1050
Percent Elongation	242%	414%	625%
Specific Gravity	1.29	N/A	1.13

Table 1: Physical properties of candidate seal materials

5.2 Compression Set Test

The compression set test provided a measurement of the amount of permanent deformation due to chemical processes caused by compression.

5.2.1 Compression Set of As-Received Elastomeric Seals

The results reported here are for elastomers tested in the as-received condition, i.e., no exposure to the simulated space environment. Measurements were taken with micrometers before the compression set test and 30-minutes after the completion of the test, and results were reported as the median value of three test specimens per ASTM Standard D395.

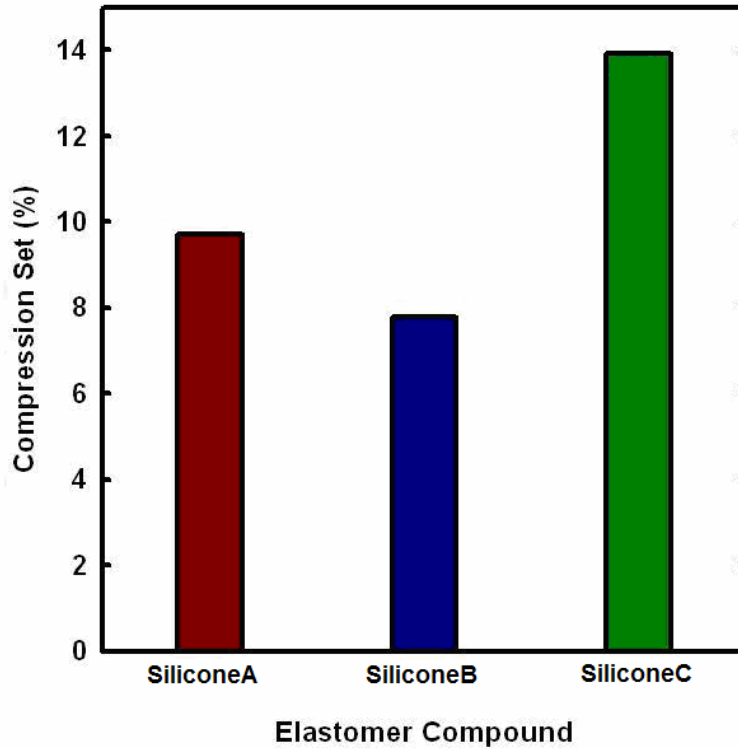


Figure 18: Compression Set test results of o-ring specimens tested per ASTM Standard D395 (Test Method B).

Based on compression set tests only, Silicone B has the least amount of compression set in the as-received condition and would therefore be the best elastomer in terms of resiliency (leak resistance).

5.3 Adhesion Test

The adhesion test measured the degree of blocking, amount of unwanted adhesion, between two like elastomer materials. This section explains in detail the attachment method of the elastomer to the test fixture which was developed from ASTM standard D3354-96 Standard Test Method for Blocking Load of Plastic Film by the Parallel Plate Method. The adhesion test study was

done to determine effect of contact period on the adhesion test results of the material in the as-received condition, i.e., without any exposure to UV or AO, where contact period is the time that the test samples were compressed. The data for the adhesion tests was scattered. In an effort to determine the cause of the scatter optical profilometry measurements were done for each of the three silicone elastomers.

5.3.1 Adhesion Test Sample Attachment Method

A consistent and non obtrusive method for attaching the elastomer to the Adhesion Test Fixture (see Figure 13) was needed in order to produce repeatable, comparable results. Because cyanoacrylate was the favored attachment method, further research was done to determine if there was any way to maximize the bond strength between the elastomer and the metal mounting button.

Cyanoacrylates come in a variety of chemical compositions and viscosities with the most common compositions shown in Figure 19.

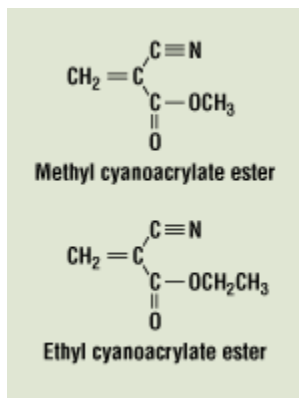


Figure 19: Chemical composition of common cyanoacrylates

Ethyl cyanoacrylates are considered to offer superior performance on plastics and elastomers over methyl-cyanoacrylates or rubber toughened cyanoacrylates. All of the cyanoacrylates used for adhesion tests were ethyl cyanoacrylates. Manufacturers cite the time required to develop certain shear strengths as the fixture speed. For example ASTM D1002 Standard Test Method for Apparent Shear Strength of Single-Lap-Joint Adhesively Bonded Metal Specimens by Tension Loading (Metal-to-Metal) defines the fixture time as the time required for the adhesive to achieve a shear strength of only 14.5psi (0.1MPa). However, cyanoacrylates typically fixture within one minute but take 24-hours to achieve their full bond strength. This finding was of significance because previous adhesion tests had only been allowed for 10 minutes before being put into compression and had frequently detached from the metal mounting button during unloading. The cure of cyanoacrylates into a rigid thermoplastic is through the presence of surface moisture. In general, if the relative humidity is below 30%, the cure rate drops dramatically. However, the relative humidity in the test facility was never below 50% in the time of operation so it was not considered in the failure evaluation of the cyanoacrylate.²⁵

Strength tests of four different cyanoacrylates were run to determine which cyanoacrylate offered the best strength for the elastomer to metal attachment. The cyanoacrylates tested were Krazy Glue®, Loctite 404, Loctite 4502, and Loctite 4861. Loctite 4502 offered the best performance based on the strength test results.



Figure 20: Photograph of 0.375in. cylindrical adhesion sample attached with cyanoacrylate

5.3.2 Effects of Hold Time

The objective of determining the effect of hold time on adhesion test results was to determine the minimum hold time that would produce results applicable to determining the maximum amount of adhesion stress between two docked spacecraft. The minimum test hold time would save money and time for the ADBS project. The method used to determine the appropriate hold time was to test the adhesion stress of the same elastomer after being held for a specific amount of time. It was optimal to test the same specimen repeatedly because of the scatter that had been seen in previous adhesion tests. The variability due to the sample was greater than variability due to load cycling.

It was predicted that after a minimum hold time the adhesion stress of the elastomer would reach a stable maximum value. It was also predicted that this minimum hold time would be material dependent. The prediction was based on the data presented in Reference []. The curves fit to the data are 3-parameter exponential fits following $y=y_o+(a- y_o)e^{-bt}$ where y_o represents the stable maximum adhesion stress between the elastomers for large values of t , b represents the exponential constant, and a is theoretical adhesion stress for very small times t . This equation was appropriate for the prediction because it incorporates a maximum adhesion stress value y_o , a minimum adhesion stress value a , and the exponential constant b which determines the time at which the adhesion stress reaches the maximum value. Fit curves were generated using SigmaPlot, a technical graphing software program. The results for each silicone elastomer are explained and presented graphically below.

In all cases, the material samples were approximately 0.20 inches (0.5cm) in thickness, compressed 25% at a rate of 0.1 in./s (0.25cm/s), held for the specified contact period, and decompressed and unloaded at a rate of 0.1 in./s (0.25cm/s). Each data curve represents the same sample being compressed repeatedly with 0.5 hours in between each test. The 25% compression was calculated based on the initial height measurements and did not factor in any compression set. The tests were ordered by increasing contact period time.

The constants for each data set using the 3-Parameter Exponential Fit are shown in the tables below each graph. The important constants to note are the b , R^2 , and t values. Although y_0 and a are important to the fit, b is the dominating factor in determining the time t at which 95% of the maximum adhesion stress will have been obtained. The R^2 value is important to note because in all cases it is above 0.95, this means that the 3-Parameter Exponential Fit follows the data very closely.

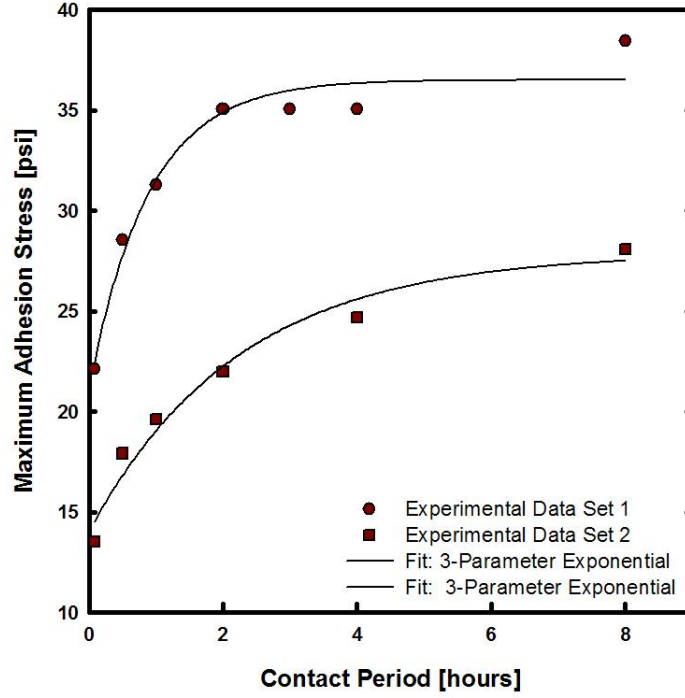


Figure 21: Effect of contact period on adhesion stress for Silicone A

	Silicone A	
	Data Set 1	Data Set 2
y_0	36.50	24.78
a	21.10	13.14
b	1.13	0.83
R^2	0.96	0.98
$y_0 - a$	15.40	11.64
t for 95% max adhesion stress (hours)	1.89	2.68
$y = y_0 + (a - y_0)e^{-bt}$		

Table 2: Experimental fit curve constants for Silicone A

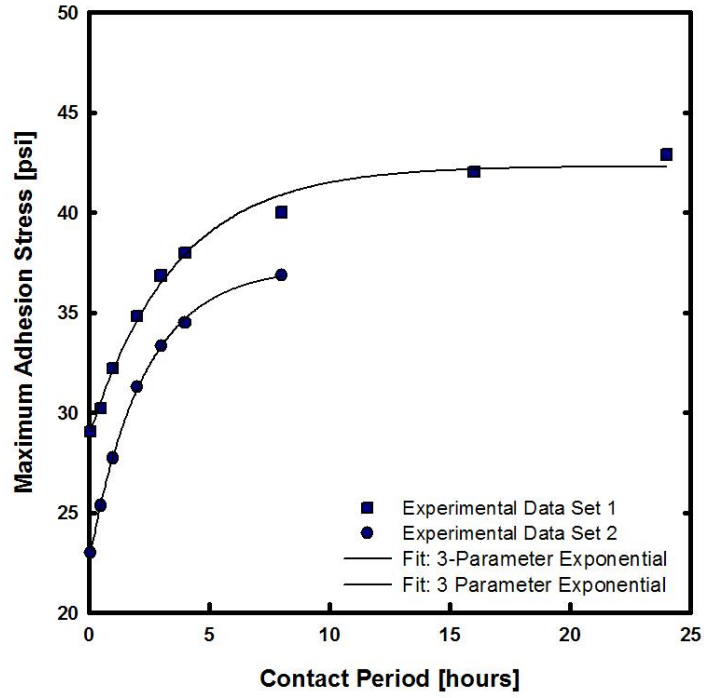


Figure 22: Effect of contact period on adhesion stress for Silicone B

	Silicone B	
	Data Set 1	Data Set 2
y_0	42.3146	37.2371
a	28.7754	22.469
b	0.2814	0.4412
R^2	0.9928	0.9996
$y_0 - a$	13.5392	14.7681
t for 95% max adhesion stress (hours)	6.60	4.69
$y = y_0 + (a - y_0)e^{-bt}$		

Table 3: Experimental fit curve constants for Silicone B

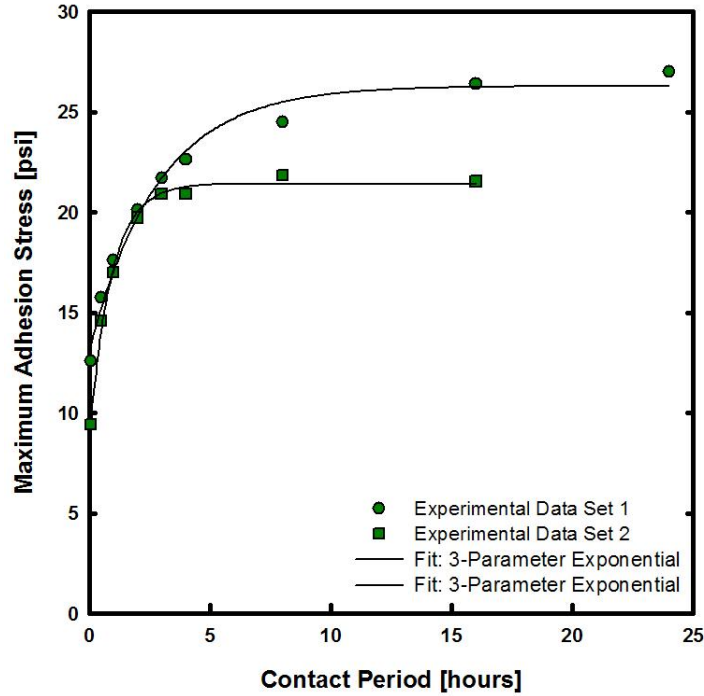


Figure 23: Effect of contact period on adhesion stress for Silicone C

	Silicone C	
	Data Set 1	Data Set 2
y_0	26.2853	20.7564
a	13.0872	8.2589
b	0.3523	1.3030
R^2	0.9829	0.9633
$y_0 - a$	13.1981	12.4975
t for 95% max adhesion stress (hours)	6.55	1.91
$y = y_0 + (a - y_0)e^{-bt}$		

Table 4: Experimental fit curve constants for Silicone C

Based on the R^2 values, a 3-Parameter Exponential Curve is accurate in predicting adhesion stress with increasing contact period. The results also show, that between data sets with in the same material there is a significant amount of scatter. This scatter is evident not only by the visual scatter from the graphs, but the time t calculated for 95% of the maximum adhesion stress

($t_{0.95}$) to be obtained. Based on these results, $t_{0.95}$ of Silicone B takes is approximately three-times that of Silicone A. The $t_{0.95}$ results of Silicone C vary too greatly to accurately compare to Silicone A or Silicone B. The exponential constant b is dominant in determining $t_{0.95}$, so although the Silicone C curves are close in value, the rate at which the two curves level out is quite different, evident from the large discrepancy in b values and therefore the large difference in the calculated $t_{0.95}$ values. However, the $t_{0.95}$ values for Silicone A and Silicone B respectively suggest that although the maximum adhesion stress obtained by each test sample pair may not be the same, the time at which it takes the test sample pair to reach its maximum adhesion stress may be the same. Using this time $t_{0.95}$ for each elastomer, test time could be minimized. It can be concluded that the amount of adhesion stress between Silicone C is less than that of Silicone A or Silicone B.

5.3.3 Summary of Effect of Contact Period on Adhesion Stress

A summary graph of the adhesion stress data is shown in Figure 24.

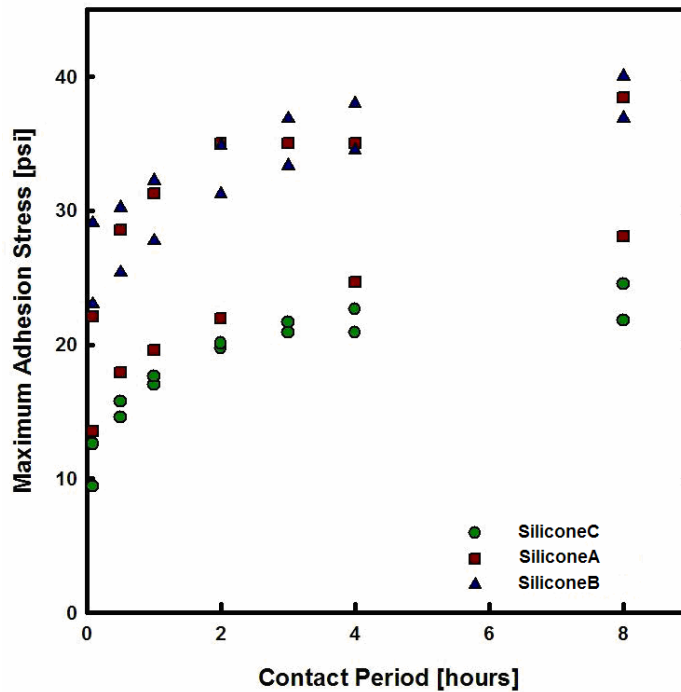


Figure 24: Comparison of effect of contact period on adhesion stress between silicone elastomers

Figure 24 shows that Silicone C has the lowest amount of adhesion stress. The results for Silicone A and Silicone B are less clear and it cannot be concluded from the graph which has a higher adhesion stress. There is more scatter in the results for Silicone A than in Silicone B. Most likely, the reason for the data scatter is because of surface variability and variability in the alignment of the two elastomer samples. As mentioned in Section 4.5, the adhesion test apparatus was designed so that the samples would be aligned, but there was still some misalignment on the order of millimeters. The steady state values, i.e., larger contact periods, are important because the space vehicles will be attached for periods of many hours, rather than minutes. However, short contact period adhesion values are also important in the prediction of the steady state values and the prediction of exponential curve.

Suggestions for further work are to continue studying the effect of contact period on adhesion stress in order to provide more data for each material and confidently predict a time $t_{0.95}$ at which the material will experience 95% of its maximum adhesion stress.

5.3.4 Optical Profilometry

In an effort to address the scatter seen in adhesion test data, an optical profilometer was used to provide a detailed contour map of the surface of each specimen. It was hypothesized that some of the scatter may have been due to the surface contour created in manufacturing. Samples were chosen from the adhesion test samples and examined with a Zygo NewView 5000 Optical Profilometer. Optical profilometry is a non-contact, three-dimensional surface profiling method which uses light interferometry. The silicone elastomer samples were not reflective enough for the microscope to profile. To solve this, gold sputter coating was used to deposit a thin gold film over the surface of the elastomer. The samples were gold-coated using a Polaron Scanning Electron Microscope (SEM) Coating Unit E5100. The sputter coating chamber is pumped down to a pressure of approximately 0.7torr or less. Sputter atoms condense on any surface they collide with, including air molecules. A low pressure allows for most of the gold atoms to condense uniformly over the surface of the sample making it reflective and visible through a light interferometry optical profilometer or SEM.

Six adhesion test sample pairs, three of Silicone A and three of Silicone B, that had already been tested in the adhesion test fixture were examined under the optical profilometer. Each sample

showed relatively the same surface contour shown in Figure 25, i.e., all surfaces deformed following a concave profile overlaid by a convex profile when rotated 90°.

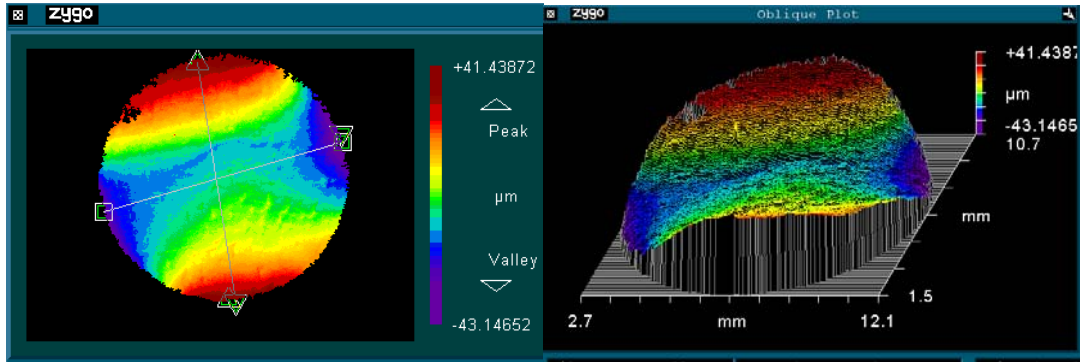


Figure 25: Silicone B sample representative of the surface contour of the adhesion samples.

The surface contour maps of Silicone A and Silicone B were too similar to draw any certain conclusions as to why the data was so scattered. The next step was to look at surface roughness and surface variability at increased magnifications of 5X and 10X.

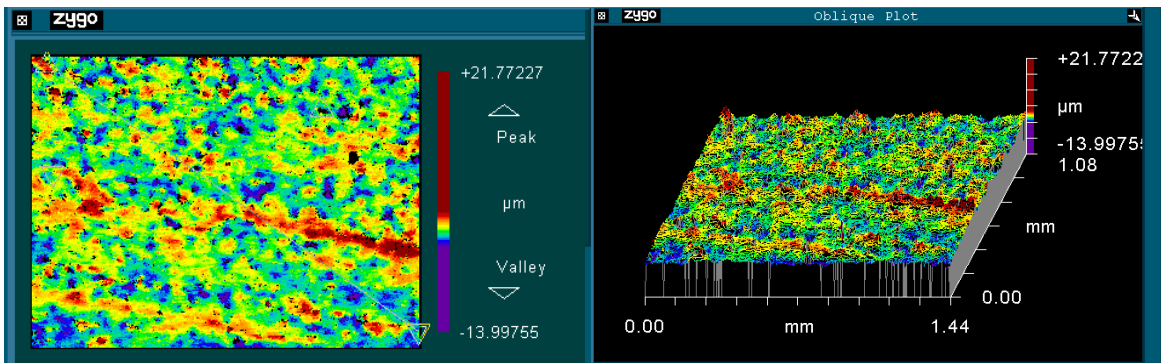


Figure 26: Silicone A optical profile at 5X magnification

Figure 26 is representative of the all three Silicone A samples that were examined under the optical profilometer. These samples were untested and in the as-received condition. The unique characteristics of the Silicone A surface profile are as follows:

- The amplitude of peak to valley is approximately $26\mu\text{m}$ ($1\text{E-}3\text{in}$);
- Peaks and valleys are globular in shape, but not necessarily circular;
- The surface is littered with linear protrusions, shown on the right side, but these protrusions are not significantly higher than the globular shaped protrusions;
- The surface roughness R_a was calculated to be $0.635\mu\text{m}$ ($2.5\text{E-}5\text{in}$) with a standard deviation $\sigma=0.133\mu\text{m}$ ($5.23\text{E-}6\text{in}$).

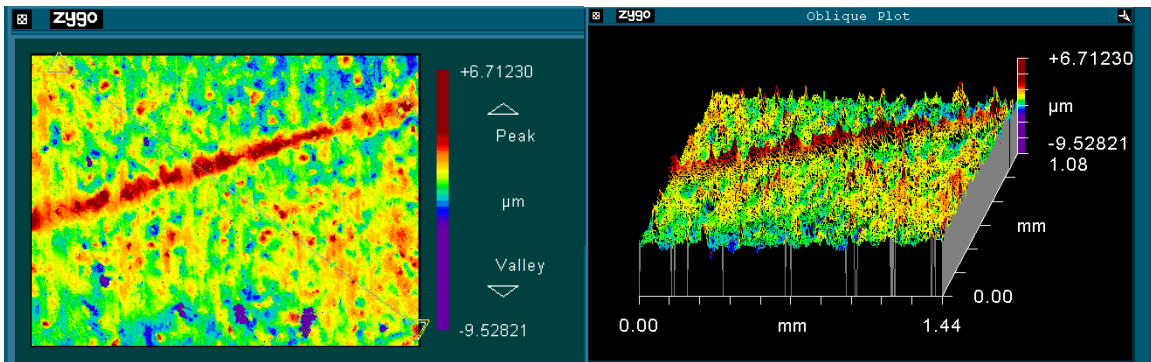


Figure 27: Silicone B optical profile at 5X magnification

Figure 27 is representative of all three Silicone B samples that were examined until the optical profilometer also in the as-received and untested condition. Although the profiles of Silicone A and Silicone B may look similar at first glance they are actually quite different from each other.

Most notably:

- The peak to valley amplitude is approximately $16\mu\text{m}$ ($6.30\text{E}10\text{-}4\text{in}$), roughly two-thirds the peak to valley amplitude of Silicone A.

- Peaks and valleys are globular in shape, but not circular in shape.
- The linear surface protrusions are significantly higher than most of the globular peaks, this is drawn from the color profile on the left of Figure 27, and more clearly from the oblique plot on the right of Figure 27.
- The surface roughness Ra was calculated to be $0.717\mu\text{m}$ ($2.82\text{E-}5\text{in}$) with a standard deviation $\sigma=0.157\mu\text{m}$ ($6.18\text{E-}6\text{in}$). This increase in standard deviation is due to the erratic distribution of the linear protrusions and their significant height increase as compared to other surface peaks.

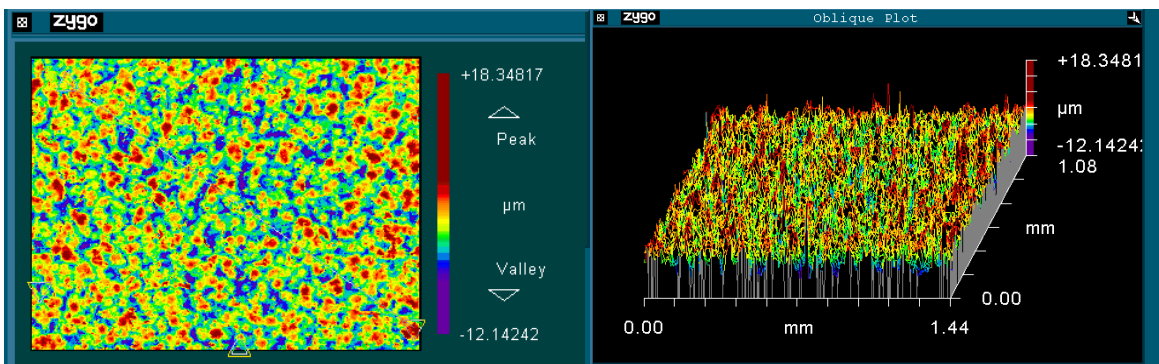


Figure 28: Silicone C optical profile at 5X magnification

Figure 28 is representative of all three Silicone C samples that were examined until the optical profilometer also in the as-received and untested condition. Recall that Silicone A and Silicone B were made by the same manufacturer, while Silicone C was from a different manufacturer.

The surface characteristics of Silicone C revealed by optical profilometry are:

- The peak to valley amplitude is approximately $30\mu\text{m}$ ($1.18\text{E-}3\text{in}$).
- The peaks and valleys are globular in shape, more circular than either Silicone A or Silicone B and are also smaller with width.

- The surface roughness Ra was calculated to be 1.936 μm (7.72E-5in) with a standard deviation $\sigma=0.063\mu\text{m}$ (2.48E-6in). The surface of Silicone C is rougher than that of either Silicone A or Silicone B, but is the most uniform.

The surface roughness measurements revealed that each material is very unique not only in composition, and hardness, but in surface texture. The very stark difference in the surface profile of Silicone A and Silicone B versus Silicone C suggest that the materials were cured, or made into 0.20inch sheets in different ways. These results suggest that the scatter in Silicone A and Silicone B could be caused by the linear surface protrusions that are found randomly on the surface of the material. The scatter in the Silicone C elastomer could be caused by the comparatively large peak to valley amplitude and smaller globular peaks and valleys. These surface profilometry measurements could also be applied to determine that likelihood that cracking will occur on the surface after exposure to AO, see Reference 18.

5.4 Durometer Results

It was hypothesized that the exposure to AO would have effects on many different aspects of the elastomers, including hardness. Hardness is an important parameter to consider for seal application because it will affect the load required for full compression. To test this hypothesis the hardness of the Silicone A and Silicone B was measured before and after AO exposure with a Rex Model DD-3 Digital Durometer^c. Both Silicone A and Silicone B elastomers received a fluence of 10E21 atoms/cm² (6.45E22 atoms/in²) of AO in the SPI Plasma Prep II asher, the equivalent to three years in the LEO.

^c Silicone C was not tested because it had not been received from the manufacturer at the time of testing.

The graph of Durometer measurements for two silicone elastomers, Figure 29, shows the average hardness for each elastomer before and after AO exposure. It was predicted that hardness would increase with AO exposure due to the layer of near-silica material formed by the reaction of AO and silicone. The hardness measurements before and after exposure to AO for Silicone A were very similar. In order to determine if the hardness measurements were statistically different, it was hypothesized that the average hardness before and after AO exposure was the same. By running an Analysis of Variance statistical test using MiniTab statistical software it was concluded that, there is a probability of only 29.8% that the hardness of Silicone A was unaffected by the AO exposure.

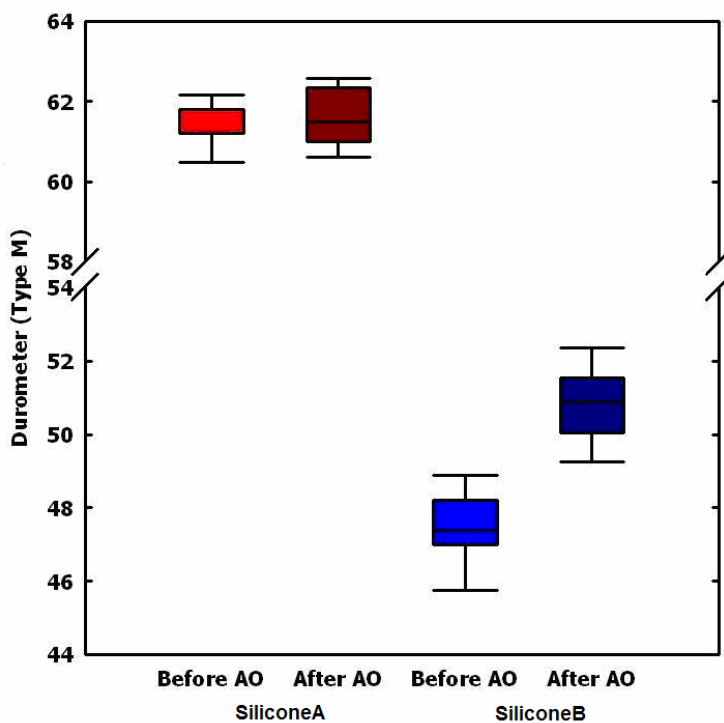


Figure 29: Durometer results for silicone elastomer compounds before and after AO exposure

In contrast, Silicone B yielded a statistically different hardness after AO exposure. No cracking could be seen on the surface of Silicone A or Silicone B but that is not to say that cracking wouldn't occur during exposure to the LEO, especially with the combined effect of UV.

6 Conclusion

In summary, three candidate silicone elastomers for use as seal material on the ADBS were evaluated for compression set in the as-received condition, adhesion stress in the as-received condition, optically profiled in the as-received condition. Two candidate silicone elastomers were Durometer tested before and after exposure to the AO.

Based on compression set test in the as-received condition only, Silicone B exhibited the best resistance to permanent compression set while Silicone C experienced the most permanent compression set.

The adhesion test results revealed that, under the test conditions specified in Section 5.3.2, all three elastomers follow an increasing 3-Parameter Exponential Curve for adhesion stress with increased contact period. Based on these preliminary results, Silicone B requires the longest amount of time to reach 95% of its maximum adhesion stress at approximately 5.5hours , while Silicone A requires the least amount of time to reach 95% of its maximum adhesion stress at approximately 2hours. The adhesion stress results for Silicone C were too varied to approximate the time for adhesion stress to reach 95% of its maximum value.

Optical profilometry results revealed very distinct surface characteristics for each silicone elastomer, as well as distinct surface characteristics between manufacturers. Potentially, the profilometry results could be combined with Durometer measurements and AO transition region measurements to predict each materials ability to resist surface cracking when exposed to AO.

The Durometer measurements support the hardness increase that would be predicted based on the formation of a near-silica surface layer after exposure to AO.

The results presented in this paper are essential preliminary results to the development of the sealing system for the ADBS. These results provide a baseline of comparison for Seals Team at NASA GRC to use after the silicone elastomers have been exposed to AO and UV. Ultimately, the seal material will be chosen based on a full data set of compression set tests, leakage tests, adhesion tests, and Durometer tests for each candidate silicone elastomer.

7 References

- ¹ E. Grossman and I. Gouzman, "Space environment effects on polymers in low earth orbit," *Nuclear Instruments and Methods in Physics Research B*, Vol. 208, 2003, pp. 48-57.
- ² Garber, S., Launius, R., Dick, S. J., & Garber, S. (2004, October 19). *A Brief History of NASA*. Retrieved May 27, 2005, from National Aeronautics and Space Administration Web site: <http://www.hq.nasa.gov/office/pao/History/factsheet.htm>
- ³ Stewart, M. (2005, April 20). *NASA - Employee Orientation*. Retrieved May 27, 2005, from National Aeronautics and Space Administration Web site: <http://employeeorientation.nasa.gov/glenn/mission.htm>
- ⁴ DeFelice, D., & Dunbar, B. (2004, December 21). *NASA – NASA FactSheet FS-2004-08-009*. Retrieved May 27, 2005, from National Aeronautics and Space Administration Web site: <http://www.nasa.gov/centers/glenn/about/fs09grc.html>
- ⁵ Oswald, J. J. (2003, February 13). *1996 Invention of the Year*. Retrieved May 27, 2005, from National Aeronautics and Space Administration Web site: http://www.grc.nasa.gov/WWW/structuralseal/InventYr/1996Inv_Yr.htm
- ⁶ Steinetz, B. M., & Oswald, J. J. (2004, January 29). *Structural Seal Website*. Retrieved Spring, 2005, from National Aeronautics and Space Administration Web site: <http://www.grc.nasa.gov/WWW/structuralseal/>
- ⁷ B.M Steinetz, M.P. Proctor, P.H. Dunlap Jr., I. Delgado, J.J. DeMange, C.C. Daniels, et al, "Overview of NASA Glenn Seal Developments," Glenn Research Center, Cleveland, OH, Nov. 2003. (NASA/CP No. 2004-212963/VOL1)
- ⁸ B.M. Steinetz, M.L. Adams, P.A. Bartolotta, R. Darolia, and A. Olsen, "High Temperature Braided Rope Seals for Static Sealing Applications," Glenn Research Center, Cleveland, OH, Nov. 1996. (NASA TM No. 107233 Revised Copy)
- ⁹ Robertson, B. (2004). *Background on Advanced Docking Berthing Systems*. Johnson Space Center. (NASA-JSC/ES5 No. 281-483-3732)
- ¹⁰ Illi, E. (1992, May 1). *Space Station Freedom Common Berthing Mechanism* (pp. 281-296) [Abstract, Electronic version]. NASA Center for AeroSpace Information (CASI). (Accession ID No. 92N25086)
- ¹¹ G. Pippin, "Space Environments and Induced Damage Mechanisms in Materials," *Progress in Organic Coatings*, Vol. 47, 2003, pp. 424-431.
- ¹² K.K. deGroh, B.A. Banks, and R. Demko, "Techniques for Measuring Low Earth Orbital Atomic Oxygen Erosion of Polymers," Glenn Research Center, Cleveland, OH, Nov. 2004. (NASA/TM No. 2002-211479)
- ¹³ B.A. Banks, K.K. deGroh, and S.K. Miller, "Low Earth Orbital Atomic Oxygen Interactions with Spacecraft Materials," Glenn Research Center, Cleveland, OH, Nov. 2004. (NASA/TM No. 2004-213400)
- ¹⁴ M.C. Lillis, E.E. Youngstrom, L.M. Marx, A.M. Hammerstrom, K.D. Finefrock, C.A. Youngstrom, et al., "Space Flight Experiments to Measure Polymer Erosion and Contamination of Spacecraft," Glenn Research Center, Cleveland, OH, June 2002. (NASA/TM No. 2002-211533)
- ¹⁵ K.K. deGroh, B.A. Banks, G.W. Clark, A.M. Hammerstrom, E.E. Youngstrom, C. Kaminski, et al., "A Sensitive Technique Using Atomic Force Microscopy to Measure the Low Earth Orbit Atomic Oxygen Erosion of Polymers," Glenn Research Center, Cleveland, OH, Dec. 2001. (NASA/TM No. 2001-211346)
- ¹⁶ K.K. deGroh, B.A. Banks, and D. Ma, "Determination of Ground-Laboratory to In-Space Effective Atomic Oxygen Fluence for DC 93-500 Silicon," Glenn Research Center, Cleveland, OH, Dec., 2004. (NASA/TM 2004-213389)
- ¹⁷ A. Snyder, B.Banks, S. Miller, T. Stueber, and E. Sechkar, "Modeling of Transmittance Degradation Caused by Optical Surface Contamination by Atomic Oxygen Reaction with Asorbed Silicones," Glenn Research Center, Cleveland, OH, June 2001. (NASA/TM 2001-210597)
- ¹⁸ C. Hung and G. Cantrell, "Reaction and Protection of Electrical Wire Insulators in Atomic-Oxygen Environments," Lewis Research Center, Cleveland, OH, 1994. (NASA/TM 1994-106767)
- ¹⁹ B.A. Banks, K.K. deGroh, S.K. Rutledge, and C.A. Haytas, "Consequences of Atomic Oxygen Interaction with Silicone and Silicone Contamination on Surfaces in Low Earth Orbit," Glenn Research Center, Cleveland, OH, May 1999. (NASA/TM 199-209179)
- ²⁰ B. Banks, S. Rutledge, E. Sechkar, T. Stueber, A. Snyder, K. deGroh, C. Haytas, and D. Brinker, "Issues and Effects of Atomic Oxygen Interactions With Silicone Contamination on Spacecraft in Low Earth Orbit," Glenn Research Center, Cleveland, OH, May 2000. (NASA/TM 2000-210056)

-
- ²¹ K.T. Gillen, M. Celina, and R. Bernstein, "Validation of Improved Methods for Predicting Long-Term Elastomeric Seal Lifetimes from Compression Stress-Relaxation and Oxygen Consumption Techniques," *Polymer Degradation and Stability*, Vol. 82, 2003, pp. 25-35.
- ²² Dunlap, P., Steinetz, B., & Daniels, C. (2005, April). *Seal Development at NASA GRC for Advanced Docking Berthing System*. Paper presented at ADBS Team Meeting at JSC.
- ²³ D3354-96 Standard Test Method for Blocking Load of Plastic Film by the Parallel Plate Method
- ²⁴ <http://www.parker.com/ead/cm2.asp?cmid=5385>
- ²⁵ P.J. Courtney and C. Verosky, "Advances in Cyanoacrylate Technology for Device Assembly," *Medical Device & Diagnostic Industry Magazine*, Sept. 1999.

Appendix A

Adhesion Test Instructions

Date: (mm/dd/yy) _____

Sample IDs: _____

Operator: _____

Sample Material

Silicone A

Silicone B

Silicone C

Other _____

Procedure

- Prepare a storage bag listing the Sample IDs and test date
- Put on finger cots or non-powdered latex gloves
- Lightly sand the gluing surface of the elastomer samples using 180 grit silicon carbide paper. Use the following sanding pattern: three vertical strokes (~3 inches in length), lifting the sample from the sand paper at the end of each stroke, so as move in the same direction (do not reverse directions). Rotate the sample 90 degrees and repeat sanding pattern, complete two more rotations and sanding patterns to cover the whole sample.

- Measure the height and diameter of the samples using calipers:

ID _____ Diameter _____ inches Height _____ inches

ID _____ Diameter _____ inches Height _____ inches

-
5. Thoroughly clean all surfaces of the samples and gluing surface of the metal mounting buttons with isopropyl alcohol
 6. Place the samples on a clean “delicate task wipe” with the test surface face down.
 7. Using Loctite 4502, place one small drop in the center of the elastomer mounting surface previously sanded. Cover the surface of the mounting button with a thin layer of Loctite 4502.
 8. Picking up the elastomer sample, press the elastomer sample and the mounting button together taking care to keep the elastomer sample aligned correctly.
 9. Press down lightly on the sample to squeeze out any excess Loctite 4502.
 10. Allow the Loctite4502 to cure for 24 hours.

Begin Cure Time: _____

End Cure Time: _____

11. Label the ID on the outer surface of each sample if it is not already labeled
12. Turn on the thermo-hydrometer now so that the reading is accurate at the start of the test.

Procedures for Adhesion Test

1. Mount the specimens in the adhesion test fixture by turning the screw threads finger tight.
2. Adjust the spacing between the specimens to about 1x the average height of the two test specimens. Clean the test surface of the elastomer samples using isopropyl alcohol on a “delicate task wipe”. Wait 10 minutes before continuing.

Begin Wait Time: _____

End Wait Time: _____

3. Open *Shortcut to ADBS Blocking Test v2.vi*

Procedures for Single Test

-
1. Choose “Run Single Test”
 2. Take care to enter the appropriate test parameters: Sample 1 Height, Sample 2 Height, Sample 1 Diameter, Sample 2 Diameter, Hold Time (s), Load Rate (in/s), Unload Rate (in/s), Compression (%), file name, as well as temperature and humidity.
Temperature _____ °F Relative Humidity _____ %

Procedures for Batch Test

1. Choose “Run Batch Test”
2. Take care to enter the appropriate test parameters: Sample 1 Height, Sample 2 Height, Sample 1 Diameter, Sample 2 Diameter, Hold Time (s), Load Rate (in/s), Unload Rate (in/s), Compression (%), file name, as well as temperature and humidity.
Temperature _____ °F Relative Humidity _____ %
3. Add batch tests as necessary using the “Add New Test” button. Parameters from the previous batch will be carried over so make sure to change the file name.
4. Place “Test in Progress” sign over the trolley and start the test.

Procedures for Stopping General of Test

1. After the batch tests are complete, remove samples, inspect them for any abnormalities, and properly store in the store bag labeled at the beginning of the test.

Procedures for Emergency Stop of Test

1. Press Emergency Stop on VI front panel.